

Contract No:

This document was prepared in conjunction with work accomplished under Contract No. DE-AC09-08SR22470 with the U.S. Department of Energy (DOE) Office of Environmental Management (EM).

Disclaimer:

This work was prepared under an agreement with and funded by the U.S. Government. Neither the U. S. Government or its employees, nor any of its contractors, subcontractors or their employees, makes any express or implied:

- 1) warranty or assumes any legal liability for the accuracy, completeness, or for the use or results of such use of any information, product, or process disclosed; or
- 2) representation that such use or results of such use would not infringe privately owned rights; or
- 3) endorsement or recommendation of any specifically identified commercial product, process, or service.

Any views and opinions of authors expressed in this work do not necessarily state or reflect those of the United States Government, or its contractors, or subcontractors.

We put science to work.™



**Savannah River
National Laboratory™**

OPERATED BY SAVANNAH RIVER NUCLEAR SOLUTIONS

A U.S. DEPARTMENT OF ENERGY NATIONAL LABORATORY • SAVANNAH RIVER SITE • AIKEN, SC

Electroless Plated Nanodiamond Coating for Stainless Steel Passivation

Dien Li

Paul S. Korinko

William A. Spencer

Edward A. Stein

September, 2016

SRNL-STI-2016-00420, Revision 0

SRNL.DOE.GOV

DISCLAIMER

This work was prepared under an agreement with and funded by the U.S. Government. Neither the U.S. Government or its employees, nor any of its contractors, subcontractors or their employees, makes any express or implied:

1. warranty or assumes any legal liability for the accuracy, completeness, or for the use or results of such use of any information, product, or process disclosed; or
2. representation that such use or results of such use would not infringe privately owned rights; or
3. endorsement or recommendation of any specifically identified commercial product, process, or service.

Any views and opinions of authors expressed in this work do not necessarily state or reflect those of the United States Government, or its contractors, or subcontractors.

Printed in the United States of America

**Prepared for
U.S. Department of Energy**

Keywords: *Nanodiamond, Electroplating, Stainless Steel, Surface Passivation*

Retention: *Permanent*

Electroless Plated Nanodiamond Coating for Stainless Steel Passivation

Dien Li

Paul S. Korinko

William A. Spencer

Edward A. Stein

October 2016

Prepared for the U.S. Department of Energy under contract number DE-AC09-08SR22470.

REVIEWS AND APPROVALS

AUTHORS:

Dien Li, Environmental Science and Biotechnology Date

Paul S. Korinko, Material Sciences and Technology Date

William A. Spencer, Analytical Department Date

Edward A. Stein, Defense Programs Technology Date

TECHNICAL REVIEW:

Dale A. Hitchcock, Materials Science and technology Date

APPROVAL:

John J. Mayer, Manager Date
Environmental Sciences and Biotechnology

Justin E. Halverson, Manager Date
Materials Science and Technology

Blythe A. Ferguson, PDRD Program Manager Date
Tritium Operation Projects

ACKNOWLEDGEMENTS

This work was supported by Plant Directed Research & Development (PDRD) Program within Savannah River Tritium Enterprise, Savannah River Nuclear Solution LLC. Work was conducted at Savannah River National Laboratory (SRNL) under the U.S. Department of Energy Contract DE-AC09-08SR22470.

EXECUTIVE SUMMARY

Tritium gas sample bottles and manifold components require passivation surface treatments to minimize the interaction of the hydrogen isotopes with surface contamination on the stainless steel containment materials. Conventional passivation processes using chemical and electrochemical means are usually insufficient to passivate tritium containment vessels and piping. Previous work demonstrated that both nitric acid and citric acid passivation on stainless steel would not prevent the catalyzed isotope exchange reaction $H_2 + D_2 \rightarrow 2HD$, while electropolishing passivation resulted in surfaces that did not catalyze this hydrogen isotope exchange. The current vendor for surface passivation treatment, Tek-Vac Industries Inc., provided the best passivation technology for the stainless steel components used at SRTE. However, this vendor recently built gas sample bottles that failed to meet site criteria and has since ceased operations. The loss of this vendor created a source gap, as well as a knowledge gap. A practical and reliable robust process to develop tritium passive surfaces is needed.

The need for alternative processes to the proprietary Tek-Vac process encouraged Savannah River Tritium Enterprise (SRTE) to pursue several passivation options. This document summarizes the effort to evaluate electroless plated nanodiamond coatings as a passivation layer for stainless steel. In this work, we developed an electroless nanodiamond (ND)-copper (Cu) coating process to deposit ND on stainless steel parts with the diamond loadings of 0%, 25% and 50% v/v in a Cu matrix. The coated Conflat Flanged Vessel Assemblies (CFVAs) were evaluated on surface morphology, composition, ND distribution, residual hydrogen release, and surface reactivity with deuterium.

For as-received Cu and ND-Cu coated CFVAs, hydrogen off-gassing is rapid, and the off-gas rates of H_2 was one to two orders of magnitude higher than that for both untreated and electropolished stainless steel CFVAs, and hydrogen and deuterium reacted to form HD as well. These results indicated that residual H_2 was entrapped in the Cu and ND-Cu coated CFVAs during the coating process, and moisture was adsorbed on the surface, and ND and/or Cu might facilitate catalytic isotope exchange reaction for HD formation. However, hydrocarbons (i.e., CH_3) did not form and did not appear to be an issue for the Cu and ND-Cu coated CFVAs. After vacuum heating, residual H_2 and adsorbed H_2O in the Cu and ND-Cu coated CFVAs were dramatically reduced. The H_2 off-gassing rate after the vacuum treatment of Cu and 50% ND-Cu coated CFVAs was on the level of 10^{-14} 1 mbar/s cm^2 , while H_2O off-gas rate was on the level of 10^{-15} 1 mbar/s cm^2 , consistent with the untreated or electropolished stainless steel CFVA, but the HD formation remained.

The Restek EP bottle was used as a reference for this work. The Restek Electro-Polished (EP) bottle and their SilTek coated bottles tested under a different research project exhibited very little hydrogen off-gassing and unmeasurable HD formation. ND and Cu were initially chosen to develop improved passivation technology, because Cu has a lower permeability of hydrogen, and diamond is more inert than other materials under a hydrogen atmosphere. However, our tests demonstrated that even after an 8-18 day vacuum extraction heat treatment, the electroless plated Cu and ND-Cu coated stainless steel CFVAs exhibited H_2 off-gassing rates that were just comparable to those for the untreated or electropolished stainless steel CFVA, and the HD formation was still observed. Thus, the Restek Electro-Polished (EP) bottle outperformed the electroless plated Cu and ND-Cu coated stainless steel CFVAs, and the electroless plated nanodiamond coating is not promising as a surface passivation technology. However, the ND-Cu coating may be beneficial to another application in which catalyzing the H_2 - D_2 exchange reaction is desired.

TABLE OF CONTENTS

LIST OF TABLES	viii
LIST OF FIGURES	viii
LIST OF APPENDIX	viii
LIST OF ABBREVIATIONS	ix
1.0 Introduction	1
2.0 Experimental Procedure	2
2.1 Plating processes for ND coatings	2
2.2 SEM and EDX Characterization	3
2.3 Vacuum Heat Treatment	3
2.4 Gas CFVA Evaluations and Mass Spectrometry	4
3.0 Results and Discussion	5
3.1 Characterization of NDs	5
3.2 Physical Appearance of the Plated Parts	6
3.3 Surface Morphology of ND-Coated Conflat Flange	7
3.4 Chemical Composition and ND Distribution of ND-Coated Conflat Flange	10
3.5 Gas Characterization of as-Received Cu and ND-Cu Coated CFVAs	12
3.6 Vacuum Heat Treatment of Cu and ND-Cu Coated CFVAs	15
3.7 Gas Characterization of Vacuum Heated Cu and ND-Cu Coated CFVAs	16
4.0 Conclusions	19
5.0 Recommendations, Path Forward and Future Work	20
6.0 References	21
7.0 Appendix I: Off-gas Rate Datasheet for Cu and ND-Cu Coated Gas CFVAs and Other Reference CFVAs	22

LIST OF TABLES

Table 2-1. Stainless Steel Parts plated at Engis Corporation.....	3
Table 3-1. Impurities Detected in the 65 nm Nanodiamond Used for Plating.....	5
Table 3-2. Gas Compositions Monitored of the as-Received Cu and ND-Cu Coated CFVAs after 7 days.	13
Table 3-3. Off-gas Rates (L mbar/s cm ²) of as Received Cu and ND-Cu Coated CFVAs Tested with D ₂ Loadings..	14
Table 3-4. Off-gas Rates (L mbar/s cm ²) of Vacuum-Treated Cu and ND-Cu Coated CFVAs Tested with D ₂ Loadings..	17

LIST OF FIGURES

Figure 2-1. Photograph of Gas CFVAs.....	4
Figure 3-1. Particle Size Distribution (PSD) of the ND used in Plating.....	6
Figure 3-2. Appearance of Cu (A), 25% ND-Cu (B), and 50% ND-Cu (C) Coated CFVAs.....	7
Figure 3-3. Discoloration Observed on 25% ND-Cu Coated Components: Flange (A) and Pipe Segment (B).....	7
Figure 3-4. SEM Images of Cu Coated Conflat Flange.....	8
Figure 3-5. SEM Images of 25% ND-Cu Coated Conflat Flange.....	9
Figure 3-6. SEM Images of 50% ND-Cu Coated Conflat Flange.....	9
Figure 3-7. Elemental Mappings of Cu Coated Conflat Flange.....	10
Figure 3-8. Elemental Mappings of 25% ND-Cu Coated Conflat Flange.....	11
Figure 3-9. Elemental Mappings of 50% ND-Cu Coated Conflat Flange.....	11
Figure 3-10. Gas Composition Profiles of the as-Received Cu and ND-Cu-Coated CFVAs after 7 days.	12
Figure 3-11. Off-gas Rates of the Key Gas Components for as-Received Cu and ND-Cu-Coated CFVAs, in Comparison with SS and EP_SS CFVAs, and Restek_#6 EP Bottle.....	15
Figure 3-12. The Vacuum Extraction Profiles for Cu and 50% ND-Cu Coated CFVA Components (A) and 25% ND-Cu Coated CFVA component (B).	16
Figure 3-13. Off-gas Rates of the Key Gas Components for Vacuum Treated Cu and 50% ND-Cu Coated CFVAs, in Comparison with SS and EP_SS CFVAs, and Restek_#6 EP Bottle.....	18
Figure 3-14. Percentages (L mbar/s cm ²) of H ₂ , HD and D ₂ for Vacuum Treated Cu and 50% ND-Cu- Coated CFVAs with H ₂ -D ₂ Mix Load.....	19

LIST of APPENDIX

Appendix I. Off-gas Rate Datasheet for Cu and ND-Cu Coated Gas CFVAs and Reference CFVAs..... 22

LIST OF ABBREVIATIONS

CF	Conflat Flange
CFVA	Conflat Flanged Vessel Assemblies
CVD	Chemical Vapor Deposition
DI	Deionized
EDX	Energy Dispersive X-ray Spectroscopy
EP	Electropolishing
ICP-OES	Inductively Coupled Plasma–Optical Emission Spectroscopy
ND	Nanodiamond
MS	Mass Spectrometer / Mass Spectroscopy
PDRD	Process-Directed Research and Development
PSD	Particle Size Distribution
SEM	Scanning Electron Microscope
SecEM	Secondary Electron Multiplier
SRNL	Savannah River National Laboratory
SRTE	Savannah River Tritium Enterprise
SS	Stainless Steel

1.0 Introduction

Tritium gas processing systems use several stainless steel alloys (e.g., Types 304L, 316L, and 347) for the processing lines. In addition, many of these stainless steel alloys are used to make 1) tubes leading from sample points in the process to mass spectroscopy systems, 2) the inlet manifolds and systems for these mass spectrometers, and 3) hydrogen isotope calibration standard bottles. These components are often passivated to prevent the stainless steel surfaces from catalyzing hydrogen migration and reactions with nitrogen, carbon, etc. in the stainless steel and to resist residual hydrogen in the stainless steel from diffusing into the vessel interior and contaminating the gas. Industrial surface passivation processes include nitric acid passivation, citric acid passivation, and electropolishing [1-3]. Tests of containers treated with these processes have not provided the same level of passivation that was achieved by the current vendor a small company called Tek-Vac Industries Inc. Recently Tek-Vac has built a number of gas sample bottles that do not meet site criteria and has subsequently ceased operations. Thus, SRNS needs to develop a reliable and robust stainless steel passivation treatment and to understand the properties that enable the surfaces to be “passive”.

Previous research has been conducted at Savannah River National Laboratory (SRNL) and Savannah River Tritium Enterprise (SRTE) to evaluate alternative commercial passivation technologies. For example, it has been demonstrated that the nitric acid and citric acid passivation processes do not prevent the isotope exchange reaction $H_2 + D_2 \rightarrow 2HD$ which is an indicator of improved performance for tritium service. The electropolished passivation process resulted in surfaces that were less likely to catalyze this hydrogen isotope exchange reaction [4]. More recently, test containers that were surface passivated by five different vendors (Tek-Vac, three vendors using electropolish/acid clean/water rinse processes, and one vendor using chemical vapor deposition (CVD) of silicon) were loaded with tritium and evaluated by monitoring impurity in-growth into the gas over time. The results indicated that 1) the only observed impurities in the gas were some HT, less CT4, and very small amounts of T_2O in all cases, 2) the current vendor (Tek-Vac) treated containers contained the fewest impurities, and 3) the CVD silicon treatment resulted in the highest impurity levels [5]. The electropolishing treatment appeared to generate a chromium oxide (Cr_2O_3) layer in thickness of 0.7-4 nm, while the CVD silicon coating appears to be SiO_2 with a thickness of ~200 nm [6]. However, a knowledge gap remains as to the mechanism for “passivation”, and it has been demonstrated that practical and robust technologies are not readily available. There was a difference in the tritium testing between the preferred treatments and the tested treatments but it was at most a factor of 2, not orders of magnitude.

An alternative material and process for passivation are of interest and that leads SRNL to consider using nanodiamond (ND) encapsulated in a metal matrix. The rationale for this composite coating as a viable passivation layer follows. Diamond is the hardest and, at low temperature, most stable material known. It is stable against various chemicals and radiation attack (including beta particles) [7]. In fact, diamonds have been investigated as radiation detectors [7,8]. Although hydrogen radicals may diffuse into its first 4-5 atomic layers [9], diamond is more inert than other materials under a hydrogen atmosphere, and its surface reactivity is less than 1% of that of graphite [10]. Based on these characteristics it was hypothesized that ND coatings on the stainless steel parts might be more reliable and enduring than the current electrochemical passivation processes due to its mechanical and chemical stability. In addition, a passive ND coating requires a suitably less reactive matrix material, and copper was chosen, because Cu has a lower permeability of hydrogen and it was the only non-nickel surface that Engis (Wheeling, IL) was willing to plate. Electroless copper was plated with the ND to prepare the ND passivation coating. This layer will act as a barrier between the substrate and gas. A thorough investigation to determine the appropriate attributes and characteristics was needed.

In this project, we investigated an electroless copper plated nanodiamond (ND) coating as a stainless steel treatment. Diamond loadings of 0%, 25% and 50% were targeted for this project. The ND coated stainless steel parts (i.e., Conflat vacuum components) were evaluated on surface morphology, composition and ND distribution, internal hydrogen release, surface reactivity with deuterium, and hydrogen isotope exchange.

2.0 Experimental Procedure

2.1 Plating processes for ND coatings

The ND coating was comprised of three main material components. The first was a nickel strike and was plated in a Wood's nickel strike plating bath and was used as a base layer to promote adhesion of copper to the type 304L stainless steel. The bath make-up was low nickel metal and high acid content. The second component was an electroless copper. For this layer, the Accu-Labs 855 Electroless Copper plating process was used. The solution is a mixture of two proprietary components, 855-M and 855-A, as well as small percentages of liquid caustic soda (50% High Purity) and formaldehyde (37% High Purity) in deionized (DI) water. Another proprietary component, 855-R acts as a replenishment to replace the copper and activator components consumed during the electroless plating process. The third component was nanodiamond (ND). The 65 nm ND used in this project was acid cleaned, and suspended in the copper plating solution to create the electroless copper-ND composite coating. The elemental impurities of this ND were analyzed using Inductively Coupled Plasma–Optical Emission Spectroscopy (ICP-OES), and its particle size distribution (PSD) was analyzed using CPS Disc Centrifuge Nano Particle Size Analyzer.

The experimental approach for this coating application included steps to ensure that the stainless steel parts were acid cleaned, and NDs are then co-deposited with Cu matrix on the desired surfaces (e.g., tube interior) of Type 304L stainless steel Conflat vacuum components through electroless plating while the other surfaces are masked. Additionally, acetone was used to clean any oils on surface of the parts. Masking tape was used to mask critical knife seals on different parts and the parts were fixtured to prevent moving during plating. The parts were then cleaned using a mild abrasive cleaner and soft scotch-brite pads in water to ensure that no water-breaks were present. After cleaning, the parts were placed on steel hooks and hung in the Wood's nickel strike solution. The parts were first etched in reverse polarity in the Wood's nickel before the current was reversed and a thin layer of nickel strike was deposited over the entire part. Following the nickel strike, the parts were rinsed thoroughly in clean running DI water and immersed in the electroless copper plating solution. The parts were plated for a period of 60 minutes in plating solution containing sufficient diamond concentration to create the desired concentration (0%, 25% and 50% ND in Cu) in the deposit. The parts were then removed and rinsed again with clean running DI water before they were dried using compressed air, and the masking was removed and the parts were cleaned again as necessary. Finally, the external surfaces were plated with Cu for appearance sake.

The stainless steel assemblies were comprised of a standard 304L 125 mm 275-150-N nipple with a blank flange on one end and a Conflat flange (CF) to VCR adapter on the other, copper gaskets were used for seals; the vessels have a nominal volume of 100 ml. The stainless steel parts, as summarized in Table 2-1, were provided by SRNL and electrolessly plated in the ND-Cu plating bath by the contracted vendor (Engis Corporation). The coated stainless steel parts were subsequently characterized using various analytical methods. Gas containing Conflat Flanged Vessels Assemblies (CFVAs) were made by assembling the nipple and flanges using copper gaskets and stainless steel bolts. The assembled CFVAs were evaluated for the surface reactivity with hydrogen and deuterium by initially evacuating the CFVAs and loading them with between 500 and 800 mTorr of deuterium gas. The gas was sampled after a week and then periodically for a period up to 110 days. A second lot of components for CFVAs was

subsequently vacuum degassed and reloaded with deuterium for a one week exposure followed by the addition of approximately 500 mTorr of protium.

Table 2-1. Stainless Steel Parts plated at Engis Corporation.

Parts	Numbers of Parts Plated with Different Nanodiamond loads in Cu matrix		
	Cu (0%)	25 %	50 %
2.75" Conflat® flanged pipe nipples, as machined	2	2	2
2.75" Conflat® flanged pipe nipples, as electropolished	2	2	2
2.75" Conflat® flanges	3	3	3
2.75" Conflat® flange to 0.25 inch VCR male adapters	2	2	2

2.2 SEM and EDX Characterization

The scanning electron microscope (SEM) used in this project was a Hitachi S3600N with an Oxford Instruments INCA Energy for Energy dispersive X-ray (EDX) spectroscopy. The Cu and ND-Cu coated flange blanks were examined as-processed to observe surface morphology by SEM-EDX. Typically, the SEM images were captured after optimizing the operational parameters (e.g., working distance, accelerating voltage and magnification) within the limits of this SEM instrument. For EDX, the spectra were collected using a voltage of 0-10 keV, optimal working distance of 15 mm and a data acquisition time of 55 seconds. X-ray mapping was also performed until adequate elemental maps were obtained.

2.3 Vacuum Heat Treatment

A vacuum tube furnace system was assembled from standard vacuum components. The hardware included two Temperature Controllers - Digi Sense 68900-11, two Over Temperature Controllers - Over-Temp Probe OTP-1800, vacuum - Pfeiffer HiCube 80 Eco, Pressure Gauge - Pfeiffer DualGauge TPG 362, and RGA - AMETEK Dycor Dymaxion Residual Gas Analyzer. The software included Temperature/Vacuum Pressure monitoring - Labview 15.0, and RGA monitoring - Dycor System 2000. A nominal 4 inch tube furnace system was assembled from commercially available stainless steel Conflat vacuum components. The heating system used pressure feedback to control the temperature within a narrow band of pressures, and a LabView program was written to control the temperature controllers on the vacuum furnace. A dead band was programmed in the Pfeiffer Dual Gauge to open the circuit to the relay for the heaters when pressure exceeded 1.0×10^{-6} Torr and to close the circuit after the pressure dropped below 9×10^{-7} Torr. This furnace system was used to extract intrinsic hydrogen entrapped in Cu, 25% and 50% ND-Cu coated 2.75" Conflat flanged pipe nipples and CF flanges. After loading and prior to heating, vacuum pressure was allowed to pull down to $<4.0 \times 10^{-8}$ Torr. Typically it took ~24 hrs to achieve the target vacuum after initially loading the samples. During heating, vacuum pressure never exceeded 1.8×10^{-6} Torr. The vacuum extraction process was stopped after the pressure reached the low to mid 10^{-8} Torr at the target temperature of 350 °C. The samples were removed after the furnace chamber cooled to below 35°C, which took several hours. The Cu and 50% ND-Cu coated nipples were loaded into the furnace at the same time. The samples released hydrogen on heating such that it took nearly 150 hours (5.83 days) to reach the soak temperature of 350 °C. They were held for at 350 °C for ~280 hrs (11.6 days) until the pressure reached the desired value. The 25% ND-Cu nipple was loaded separately, it took approximately 74.5 hrs to ramp to 350 °C (3.1 days) and was soaked at 350 °C for ~124 hrs (5.1

days). The duration of the soak was dictated by the pressure with the goal of achieving less than 9×10^{-8} Torr or less prior to terminating the treatment.

2.4 Gas CFVA Evaluations and Mass Spectrometry

The nominal 100 cc volume CFVAs were connected to a Swagelok electropolished and cleaned stainless steel-4BG bellows valve (Figure 2-1). The internal surfaces of CFVAs were coated with Cu, 25% and 50% ND-Cu for surface passivation, as described in Section 2.1, while the external surfaces of the CFVAs were coated with Pure Cu for decorative purposes.



Figure 2-1 Photograph of Gas CFVAs

To monitor the off gas performance of each vessel, each was connected to the Pfeiffer quadrupole inlet manifold and pumped down to less than 0.01 mbar using a turbo vacuum pump on the inlet system. The bottles were allowed to sit under vacuum for 24 hours and then the mass spectrometer was used to check for air in-leakage by monitoring nitrogen and oxygen masses in each bottle. The bottles were then loaded to approximately 1 mbar with 99.8% deuterium. In a 100 mL nominal volume bottle this is equivalent to adding 100 microliters of deuterium at atmosphere (1 bar). The bottles were closed and allowed to stand on the manifold for approximately 1 week. An aliquot from the bottle was then expanded into the manifold and then to the mass spectrometer. Masses 1-65 were monitored. Additional aliquots were taken over time. The number of aliquots was limited to about 3 samples due to the lowering of pressure in the bottles with each aliquot. A mass scan of the deuterium at 1 mbar was used as a background correction signal and subtracted from the scans of each aliquot after the aliquot scans were scaled to 1 mbar equivalent pressure. This allowed the data to highlight the changes from the reference gas load and corrected data for pressure dependent background residual gas in the mass spectrometer. Offgas Data was also scaled for the calculated surface area of the vessel. Some of the bottles had a lower background than our manifold which resulted in an occasional negative number for very good results.

The mass spectrometer was a 400-5 series Pfeiffer quadrupole with a large HiPACE 400 turbo pump backed with a secondary turbo pump station. The spectrometer ran the Inficon Quadera software package and normally set to scan to mass 65 using the Secondary Electron multiplier (SeEM) detector with 1700V gain. These settings allowed the system to detect impurities at ppm levels in atmospheric pressure samples for most gases of interest. A 0.1% change in test samples was easily observed and equivalent to 1 ppm for nitrogen or carbon monoxide at atmospheric pressure. Sensitivity for hydrogen was approximately twice that of nitrogen, but deuterium was equivalent to nitrogen. Mass resolution was set

for 0.5 amu. The system was set to continuously scan and store data during measurements. Spectrometer pressure was measured using a Pfeiffer PB-260 full range gauge with a hot cathode. Post processing of the data with Excel allowed for extrapolating concentrations to load zero time and accounting for pumping diffusion rates. System background was limited by the rhenium filaments. The filaments emitted oxygen, Rh^{2+} , and Rh^+ as well as several trace hydrocarbon and alkali impurities depending on the filament batch. Hydrogen, water, carbon monoxide, and carbon dioxide were also present in background spectra. The spectrometer was mounted in an aluminum housing for vacuum containment which helped maintain a low system hydrogen and water background. A small SAES D100 ion getter pump assisted pumping of hydrogen.

Actual measurements were made by collecting a gas sample aliquot from the test CFVA or bottle to give a deuterium reading of approximately 2×10^{-7} mbar on the spectrometer pressure gauge. Typical ion currents were from 5×10^{-7} amps to 2×10^{-13} amps, which were the sample deuterium peak current and the electronic noise floor for the SecEM. Individual ion backgrounds increased the instrumentation limit for several ion lines and background was somewhat pressure dependent. The background level from a new deuterium aliquot was used to correct sample measurements for system background. The sample pressure was designed to limit the pressure-dependent formation of D^{3+} , H^{3+} , HD^{2+} , and D_2H^+ within the ion source. Sample pressure for ultra-trace measurements could be raised to 1×10^{-5} amps with some protonation or deuteration observed.

3.0 Results and Discussion

3.1 Characterization of NDs

The elemental impurities of this ND were analyzed using extrinsic and intrinsic methods. The extrinsic impurities are the impurities on the diamond surfaces. These were measured by acid washing the diamond and analyzing dissolved elements in the solutions using ICP-OES. The intrinsic impurities are those found within the diamond. That was done by 1) acid washing the diamond to remove the extrinsic impurities, 2) digesting the diamond, 3) measuring the elemental concentrations of the resulting solution using ICP-OES. The elemental impurities of NDs used for these coatings are given in Table 3-1. The contents of these elements met the internal specification of NDs for quality control at Engis. The extrinsic concentrations of Na, Fe and Mn on the ND surfaces are fairly high compared to other elements, while the major intrinsic impurities of this ND are Fe (~70 ppm), and to lesser extent Mn (~7 ppm). Since ND was acid cleaned before being added into the Cu electroless bath solution, the major impurities of the ND in the coatings are Fe and Mn. It is unknown whether or how the intrinsic impurities (especially Fe) of the ND would impact the passivation behavior of ND-Cu coated stainless steel parts.

Table 3-1. Impurities Detected in the 65 nm Nanodiamond Used for Plating.

Lot #	Sample #	Method	Elemental Impurities (ppm)										
			B	Co	Fe	Mn	Na	Ni	Si	Cr	Cu	Mg	Total
R0440	1	extrinsic	1	0	154	49	1230	1	7	3	1	5	1451
R0440	2	extrinsic	0	0	155	45	1086	0	8	2	2	6	1305
Average			<1	<1	154	47	1158	<1	7	2	2	5	1377

R0440	1	intrinsic	0	0	85	8	0	1	6	3	0	1	103
R0440	2	intrinsic	0	0	54	6	0	0	3	1	0	1	65
Average			0	0	70	7	0	1	4	2	0	1	84

The particle size distribution of this ND was measured using a CPS Disk Centrifuge Nano Particle Size Analyzer, and is shown in Figure 3-1. The median size of this ND is 66.5 nm.

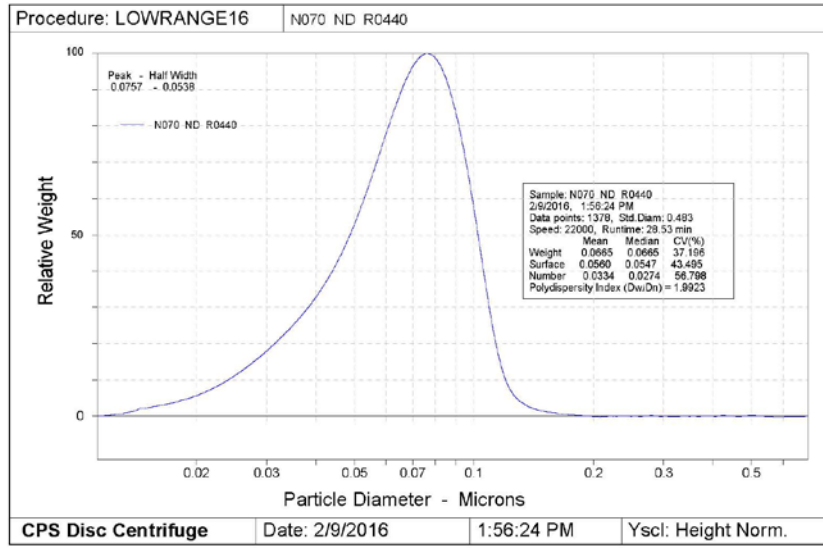


Figure 3-1. Particle Size Distribution (PSD) of the ND used in Plating

3.2 Physical Appearance of the Plated Parts

The assembled Cu and ND-Cu coated CFVA components are shown in Figure 3-2. All of these CFVA components had similar external surfaces characteristic of the pipe spool pieces, but the blank flanges and VCR to CF adapter flanges exhibited some discoloration and apparent staining (Figure 3-3). In addition to the stains and surface inconsistencies, the sheen of the coatings was also different. The pure Cu coating was more reflective while the ND-Cu coatings tended to have a matte appearance. The coated CF and VCR adapters exhibited a darker orange appearance rather than a matte appearance.

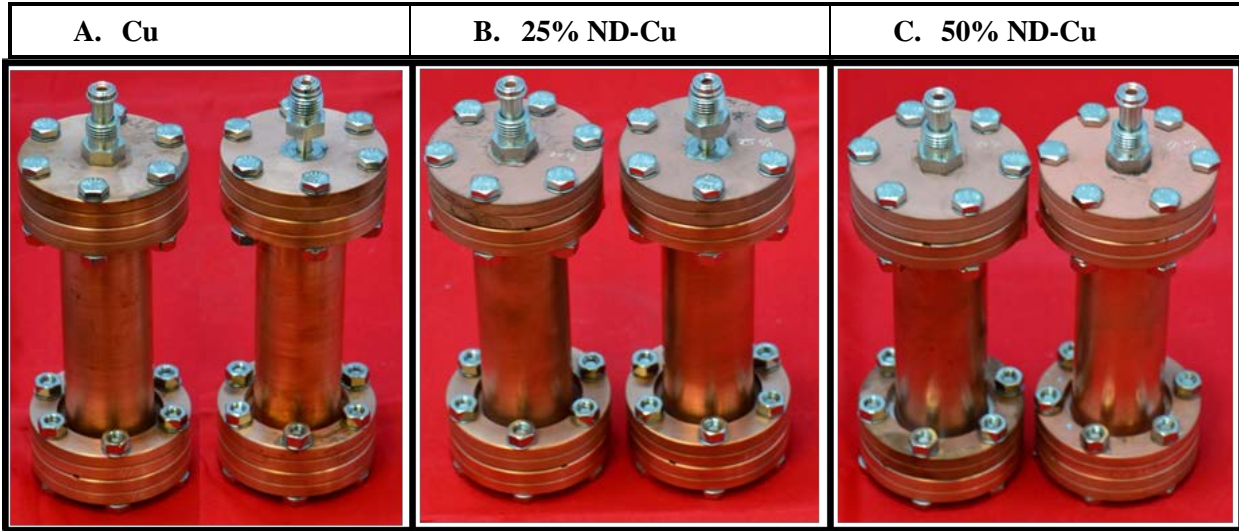


Figure 3-2. Appearance of Cu (A), 25% ND-Cu (B), and 50% ND-Cu (C) coated CFVAs.

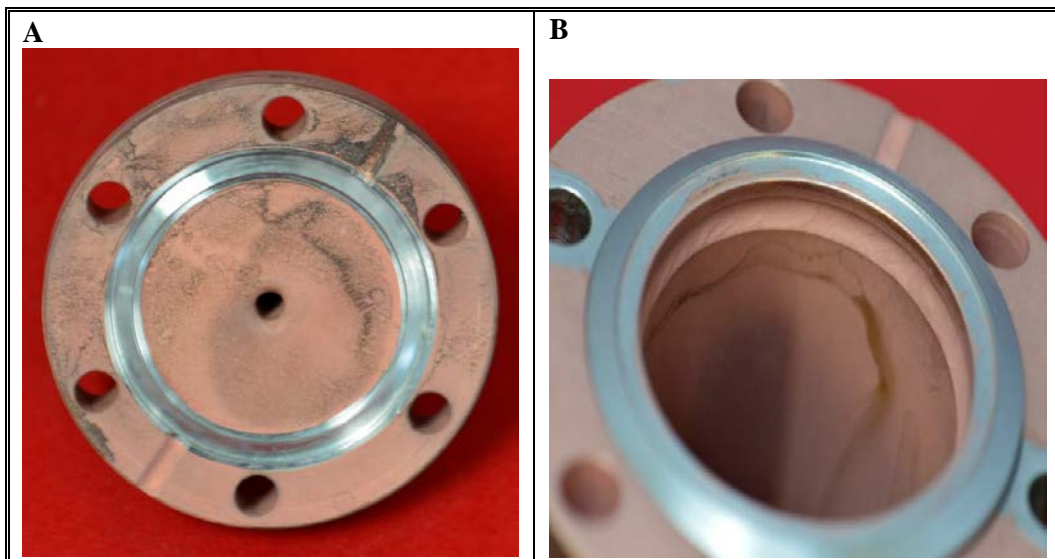


Figure 3-3. Discoloration Observed on 25% ND-Cu Coated Components: Flange (A) and Pipe Segment (B).

3.3 Surface Morphology of ND-Coated Conflat Flange

SEM images for Cu, 25% and 50% ND-Cu plated CF flange blanks are shown in Figures 3-4, 3-5, and 3-6, respectively. The Cu coating was not uniform, exhibiting some pores (e.g., Figure 3-4) or other crater-like defects (e.g., Figure 3-5). Although there was no evidence to indicate whether the stainless steel substrate was exposed or not through the pores, it appeared that some areas of the 50% ND-Cu coated nipple were not well coated by copper (Figure 3-6). The coated metallic Cu exhibited an apparent grain size of 5-10 μm . However, the size, shape and morphology of the metallic Cu varied with the ND loading.

Metallic Cu had an octahedral appearance in the absence of ND (Figure 3-4). The Cu matrix exhibits a spherical morphology when deposited in the presence of 25% ND (Figure 3-5). The Cu deposit morphology was even further modified appearing as spheres and long rods with varying sizes from 5 to 25 μm in the 50% ND-Cu coated flange (Figure 3-6). The 50% ND-Cu coated flange also exhibited a number of globules of 100 μm or larger in size on the surface.

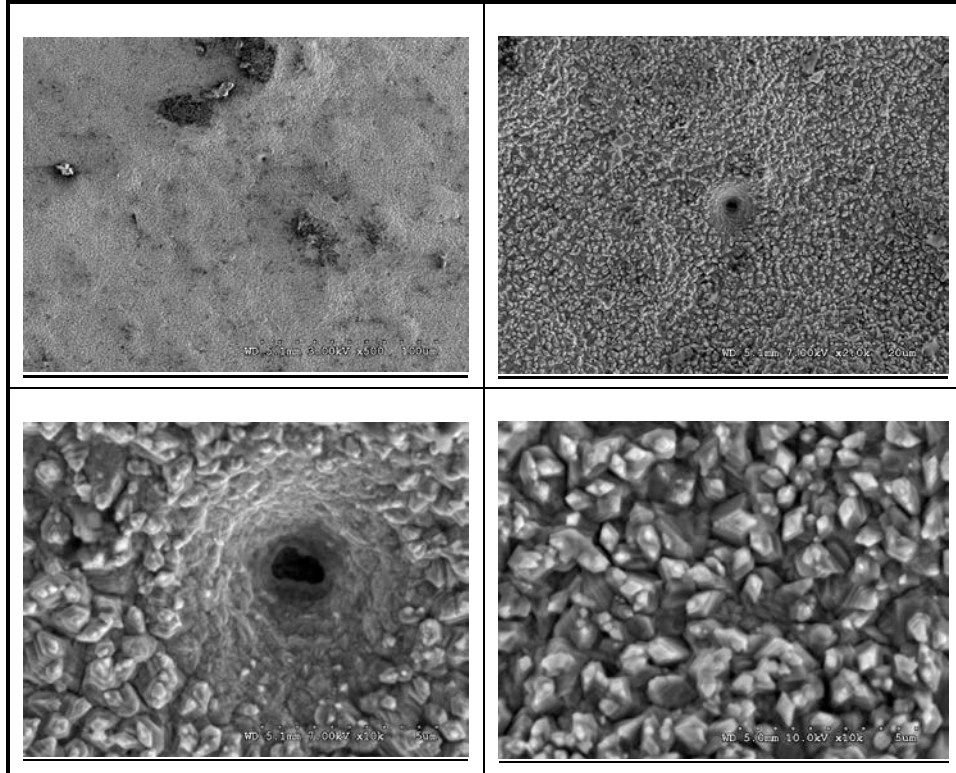


Figure 3-4. SEM Images of Cu Coated Conflat Flange.

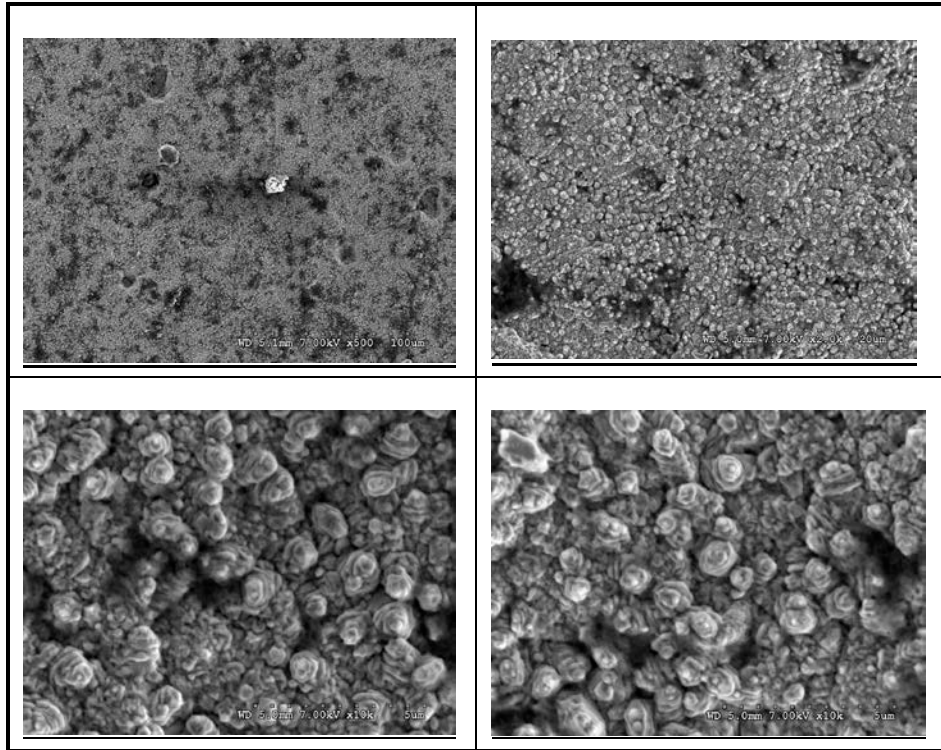


Figure 3-5. SEM Images of 25% ND-Cu Coated Conflat Flange.

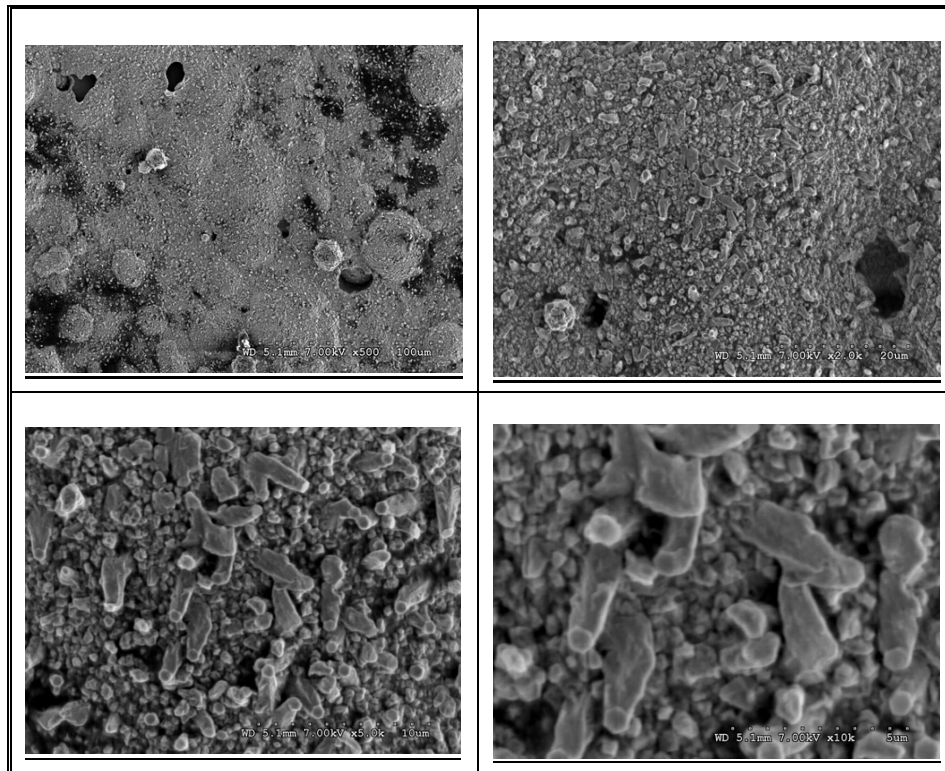


Figure 3-6. SEM Images of 50% ND-Cu Coated Conflat Flange.

3.4 Chemical Composition and ND Distribution of ND-Coated Conflat Flange

The elemental maps of Cu, 25% and 50% ND-Cu coated nipples are shown in Figures 3-7, 3-8, and 3-9, respectively. Figure 3-7 indicated that the chemical composition for the selected area is primarily Cu, while C, O, Ni and Fe are near the background levels. Also, Fe or Ni is not significantly higher at the pore area, which suggests that the coating holiday did not extend through the coating to expose the inner stainless steel substrate. Similarly, for the 25% ND-Cu coated nipple (Figure 3-8), the chemical compositions of the mapped area were primarily Cu and C while O, Ni and Fe were observed near the background. Figure 3-9 shows that the globules of the size up to 5 μm were further aggregated to the size of $\sim 50 \mu\text{m}$ in the 50% ND-Cu coated nipple. The elemental maps indicated that the globules were primarily C, presumably, the aggregates of NDs, while the surrounding areas were Cu. There are several pores or defects, but the Fe map did not show any bright spots, indicating that coating holidays did not extend through the coating to the stainless steel substrate or nickel strike.

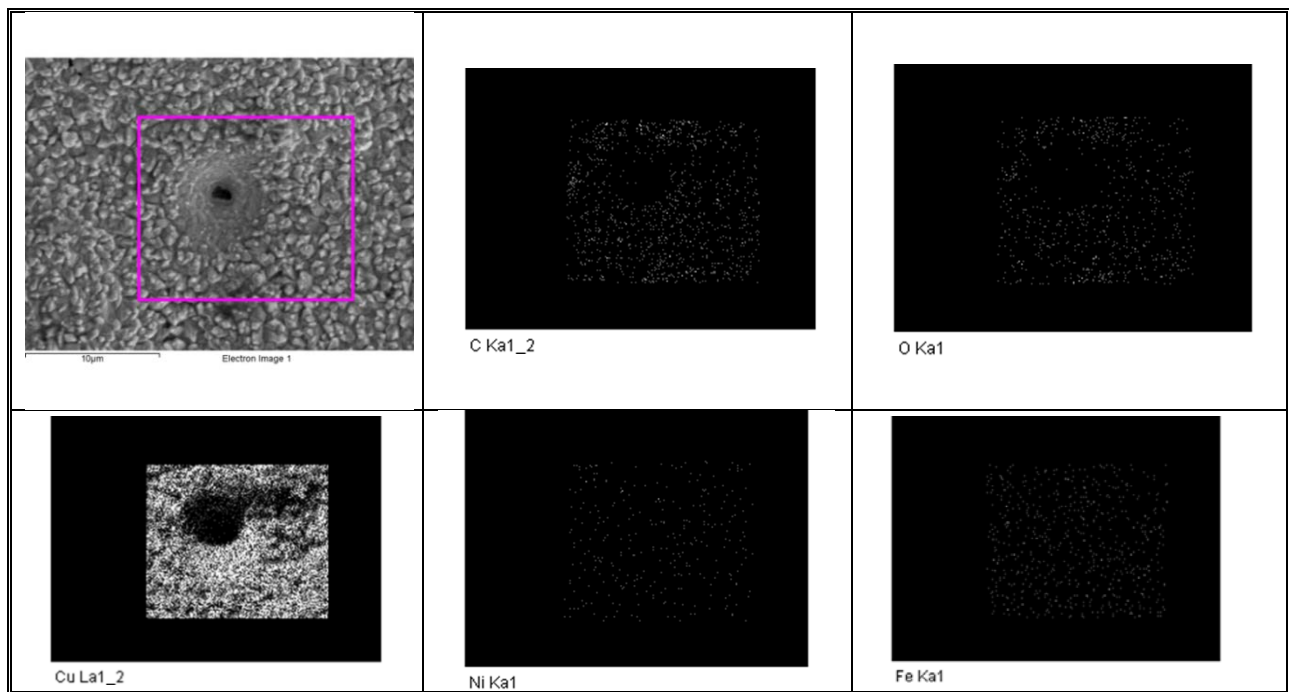


Figure 3-7. Elemental Mappings of Cu Coated Conflat Flange.

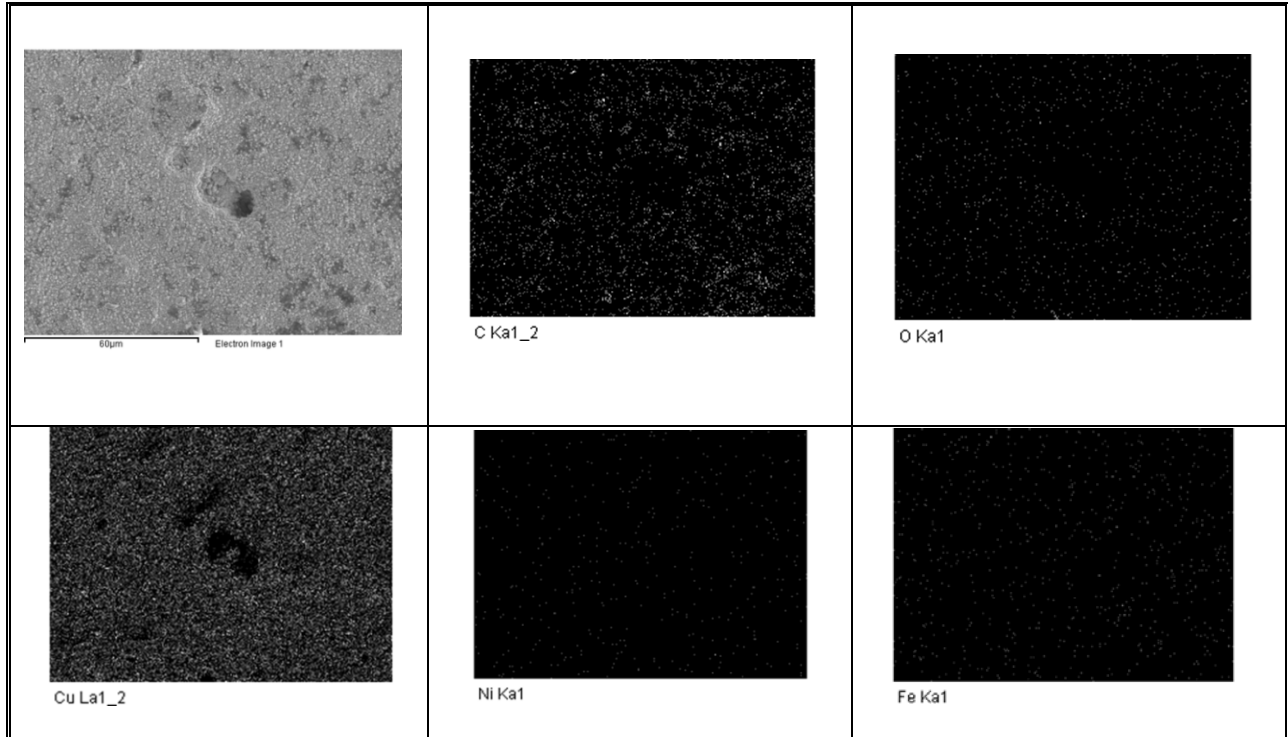


Figure 3-8. Elemental Mappings of 25% ND-Cu Coated Conflat Flange

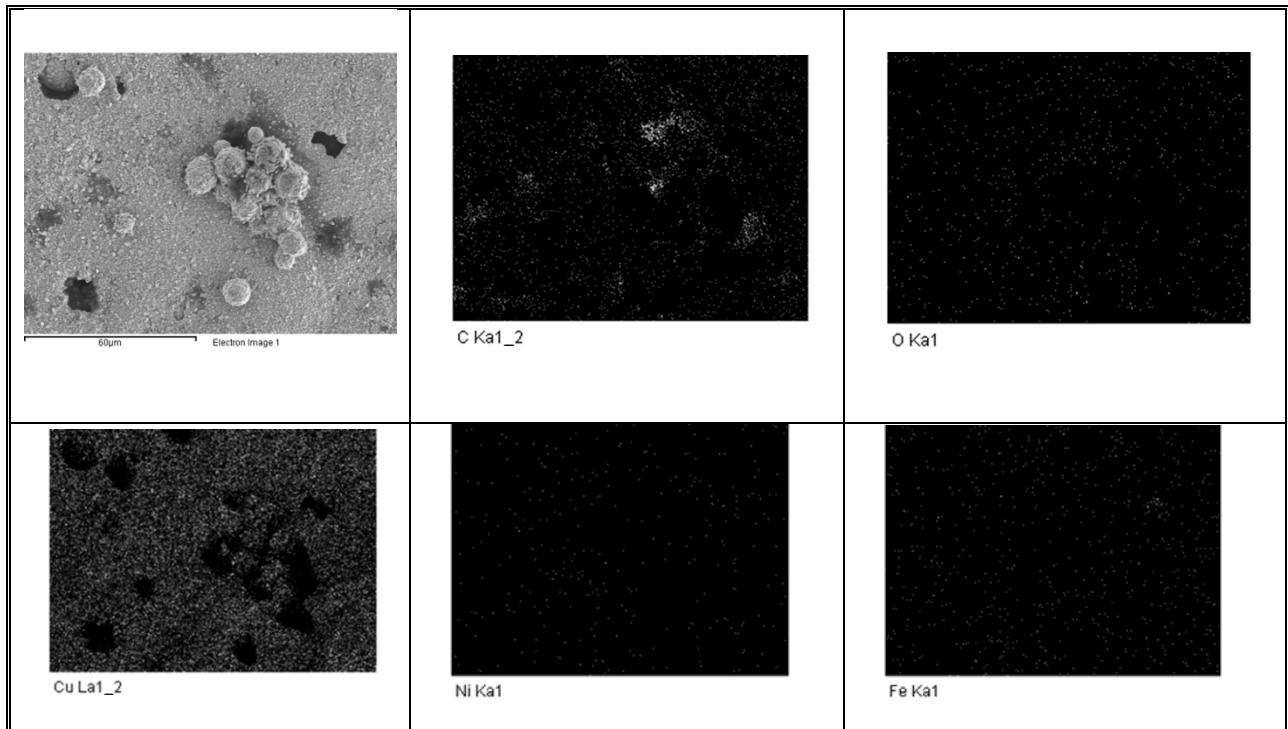


Figure 3-9. Elemental Mappings of 50% ND-Cu Coated Conflat Flange

3.5 Gas Characterization of as-Received Cu and ND-Cu Coated CFVAs

The Cu and ND-Cu coated CFVAs and a baseline CFVA were loaded with 500-800 mTorr of 99.9% deuterium. The bare and coated gas CFVAs were initially monitored using mass spectroscopy after a week exposure to D₂. The MS data were normalized as a ratio between the measured H₂ and HD ion current to the measured D₂ ion current and indirectly the gas quantities. This was done to account for the variable gas pressures that were used for loading into the CFVAs. The H₂/D₂, HD/D₂ or H₂O/D₂ ratios for the Cu and ND-Cu coated CFVAs are shown in Figure 3-10 and summarized in Table 3-1. The pressure decay is an artifact of the testing method.

An unexpectedly high H₂ in-growth was measured in the Cu and ND-Cu CFVAs, which indicated that there is a significant amount of residual hydrogen in/on the coatings, and vacuum heating / extraction is warranted for these components. However, the amount of H₂ detected is not correlated to the nominal ND loadings. The amount of H₂ measured for the 25% ND-Cu coated was significantly higher than that measured for Cu and 50% ND-Cu coated CFVAs. This result might be related to an experimental error of a valve misalignment while loading the samples. This valve misalignment resulted in the Cu and 50% ND-Cu coated CFVAs being evacuated and statically off-gassed for an additional week prior to being loaded with D₂. It is noteworthy that substantially higher HD was detected for the ND-Cu coated CFVAs than for the stainless steel CFVA, and it appeared that the amount of HD detected is qualitatively correlated with the nominal ND loadings in the CFVAs. These results may indicate that coated ND and/or Cu might catalyze the H₂-D₂ exchange equilibrium reaction, which is undesirable for the purpose of surface passivation. This result, however, may be beneficial for another application in which catalyzing the H₂-D₂ exchange reaction is desired. The amount of H₂O detected for the 25% ND-Cu CFVA was also significantly higher than that measured for the Cu and 50% ND-Cu coated CFVA in which the amount of H₂O is similar to that of the stainless steel CFVAs. These results may be related to the experimental error discussed above where the additional week in the evacuated state for the Cu and 50% ND-Cu coated CFVAs removed some of the adsorbed water.

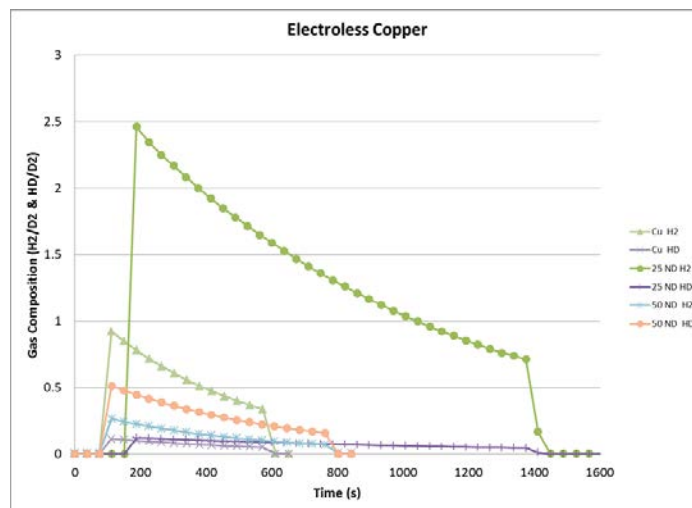


Figure 3-10. Gas Composition Profiles of the as-Received Cu and ND-Cu-Coated CFVAs after 7 days.

Table 3-2. Gas Compositions Monitored of the as-Received Cu and ND-Cu Coated CFVAs after 7 days.

Coatings on Stainless Steel (SS) CFVAs	D ₂ Pressure (mbar)	H ₂ /D ₂	HD/D ₂	H ₂ O/D ₂
Cu_SS	6.452×10 ⁻⁸	0.923	0.115	0.007
25% ND-Cu_SS	1.355×10 ⁻⁷	2.463	0.122	0.025
50% ND-Cu_SS	5.114×10 ⁻⁸	0.266	0.513	0.008
SS	1.158×10 ⁻⁷	0.017	0.042	0.005
Restek_#6 EP bottle	1.192×10 ⁻⁷	0.015	0.012	0.006

A second method to evaluate the treatment is to compare the effective off-gas rates. The gas compositions of the CFVAs loaded with D₂ were monitored and measured using a mass spectrometer (MS) at varying time intervals up to 105 days. The D₂ reference data set was subtracted from all the data that were treated as if it was deuterium. This subtraction allows most of the MS background features to be removed and to focus the spectral changes. The off-gas rates were determined by comparing the first data point from the mass spectrometer, normalizing the intensity using a standard deuterium intensity and dividing by the exposure time to calculate an off-gas rate. All data were normalized to constant ion current for 100 μL of D₂ at 1 mbar. A positive value indicates an increase in the ion compared to the starting reference condition, while a negative number reflects a decrease compared to the starting mass spectrometer background conditions, and therefore an improvement of the background signal over the reference values. The complete off-gas rate dataset is given in Appendix I.

The off-gas rates of the most important gas species (i.e., H₂, HD, H₂O, CH₃, N₂, and O₂) for the as-received CFVAs, in comparison with stainless steel (SS) and electropolished (EP) SS CFVAs, and Restek's #6 EP bottle, are given in Table 3-3 and displayed in Figure 3-11, which shows an effective off-gassing rate based on the method indicated above. Several observations can be made based on these data as follows.

Hydrogen off-gassing is rapid for the Cu and ND-Cu coatings, and the rate of hydrogen evolution at room temperature is nearly constant over the duration of these tests. Compared to untreated SS and EP_SS CFVAs, the off-gas rates of H₂, HD and H₂O were one to two orders of magnitude higher for Cu and ND-Cu coated SS CFVAs. However, there were two outliers for H₂O (Cu_SS, 7 days, and 50% ND-Cu_SS, 7 days) in which the off-gas rates were negative. In agreement with the gas composition profiles (Figure 3-10), the higher off-gas rates of H₂ and H₂O demonstrated residual H₂ was entrapped in the Cu and ND-Cu coated CFVA components, and H₂O adsorbed on the surfaces during the plating process; it is expected that these components require vacuum heat treatment to eliminate or minimize the residual H₂ and H₂O.

The off-gas rates of CH₃ for 25% ND-Cu coated SS CFVA at three different time intervals were nearly one order of magnitude higher than those for SS and EP_SS, but the off-gas rates of CH₃ for Cu and 50% ND-Cu coated CFVAs were similar to those of SS and EP_SS CFVAs, which indicated that the off-gas rate of CH₃ is not correlated with the nominal ND loadings in the Cu coatings. The off-gassing of CH₃ normally indicates the formation of hydrocarbons, which is often of a concern for tritium service. It appears that the Cu and 50% ND-Cu coated SS CFVAs were different than 20% ND-Cu and without higher levels of CH₃ formation. The higher off-gas rate of CH₃ for the 25% ND-Cu coated SS CFVA might be contributed to the experimental error of misalignment we discussed above, but it is unknown why the CH₃ off-gas rate remained constant over the course of three sampling times.

The detection of N₂ and O₂ is normally indicative of an air leak into the experimental setup. The off-gas rates of N₂ and O₂ for Cu_SS at 43 days, 25% ND-Cu_SS at 43 days, and 50% ND-Cu_SS at 36 days were about one order of magnitude higher than those for SS and EP_SS CFVAs at 12 days. The off-gas rates N₂ and O₂ for 25% ND-Cu_SS CFVA at 105 days were even nearly two orders of magnitude higher than those for SS and EP_SS CFVAs at 12 days. The off-gas rates of N₂ and O₂ appear to be related to the duration that the gas CFVAs were loaded with D₂; the longer the gas CFVAs were monitored, the higher the off-gas rates were of N₂ and O₂ and leakage was more likely. This air leak may simply be related to the experimental setup, or may be related to the integrity of the gas CFVAs. However, there is no evidence to indicate that the Cu and ND-Cu coated SS CFVAs have air leak issues compared to the SS and EP_SS CFVAs, because the off-gas rates of N₂ and O₂ were similar to each other and similar to the reference CFVAs at similar D₂ exposure.

Untreated stainless steel and electropolished stainless steel CFVAs had hydrogen off-gassing rates that were about two orders of magnitude lower than the Cu and ND-Cu, and the Restek EP and SilTek coating had very little hydrogen off-gassing and unmeasurable H₂/D₂ exchange (11).

Table 3-3. Off-gas Rates (l mbar/s cm²) of as Received Cu and ND-Cu Coated CFVAs Tested with D₂ Loadings

CFVAs	Time (Days)	H ₂	HD	H ₂ O	CH ₃	N ₂	O ₂
Cu_SS	7	98.6×10 ⁻¹⁴	11.4×10 ⁻¹⁴	-0.1×10 ⁻¹⁵	4.77×10 ⁻¹⁷	1.45×10 ⁻¹⁵	0.09×10 ⁻¹⁶
Cu_SS	43	72.6×10 ⁻¹⁴	10.7×10 ⁻¹⁴	13.0×10 ⁻¹⁵	6.19×10 ⁻¹⁷	11.4×10 ⁻¹⁵	12.1×10 ⁻¹⁶
25% ND-Cu_SS	7	266×10 ⁻¹⁴	12.1×10 ⁻¹⁴	15.2×10 ⁻¹⁵	41.8×10 ⁻¹⁷	8.26×10 ⁻¹⁵	0.24×10 ⁻¹⁶
25% ND-Cu_SS	43	326×10 ⁻¹⁴	57.1×10 ⁻¹⁴	122×10 ⁻¹⁵	47.4×10 ⁻¹⁷	18.5×10 ⁻¹⁵	11.5×10 ⁻¹⁶
25% ND-Cu_SS	105	36.9×10 ⁻¹⁴	8.99×10 ⁻¹⁴	4.37×10 ⁻¹⁵	24.9×10 ⁻¹⁷	154×10 ⁻¹⁵	195×10 ⁻¹⁶
50% ND-Cu_SS	7	26.4×10 ⁻¹⁴	53.5×10 ⁻¹⁴	-0.06×10 ⁻¹⁵	8.30×10 ⁻¹⁷	1.44×10 ⁻¹⁵	0.47×10 ⁻¹⁶
50% ND-Cu_SS	36	63.3×10 ⁻¹⁴	52.6×10 ⁻¹⁴	133×10 ⁻¹⁵	9.84×10 ⁻¹⁷	29.8×10 ⁻¹⁵	31.8×10 ⁻¹⁶
SS	12	0.84×10 ⁻¹⁴	1.96×10 ⁻¹⁴	-0.12×10 ⁻¹⁵	0.86×10 ⁻¹⁷	2.16×10 ⁻¹⁵	1.28×10 ⁻¹⁶
EP_SS	12	1.58×10 ⁻¹⁴	2.36×10 ⁻¹⁴	7.04×10 ⁻¹⁵	6.07×10 ⁻¹⁷	2.55×10 ⁻¹⁵	2.24×10 ⁻¹⁶
Restek_#6 EP	12	-0.006×10 ⁻¹⁴	0.004×10 ⁻¹⁴	-0.07×10 ⁻¹⁵	0.05×10 ⁻¹⁷	0.02×10 ⁻¹⁵	-0.008×10 ⁻¹⁶

Note: Negative numbers indicate reading was better than the reference blank deuterium standard that was used to correct the mass spectrometer background.

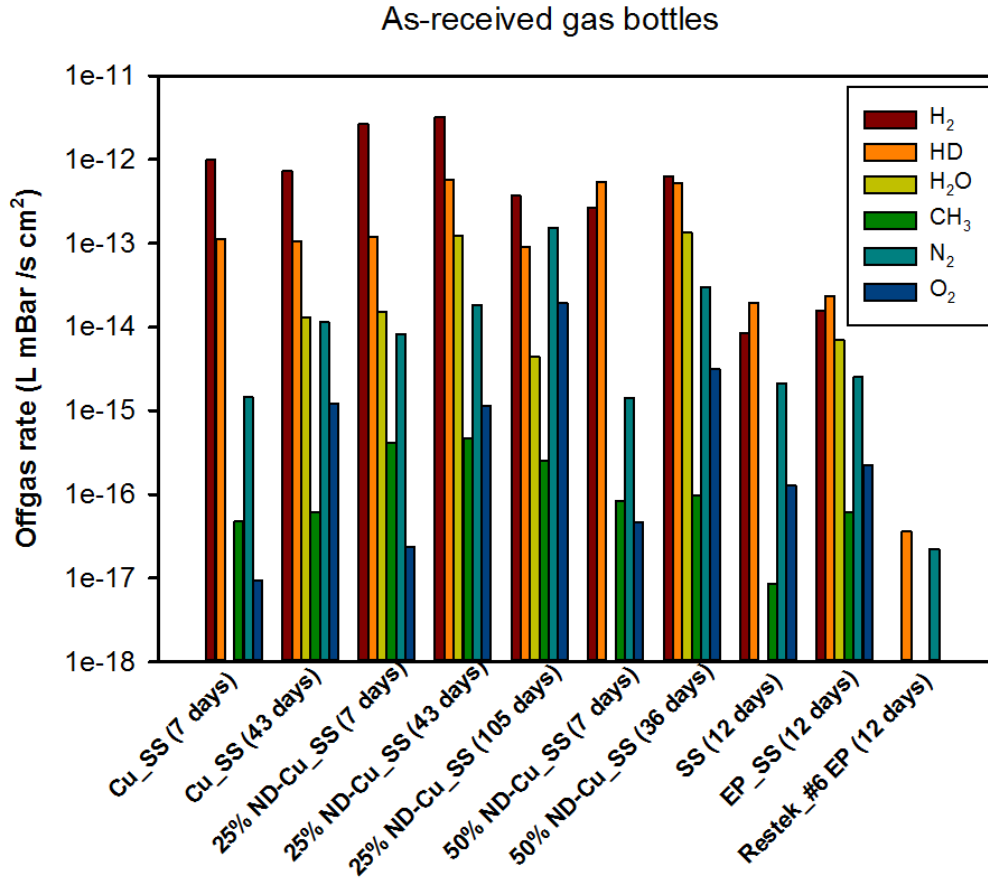


Figure 3-11. Off-gas Rates of the Key Gas Components for as-Received Cu and ND-Cu-Coated CFVAs, in Comparison with SS and EP_SS CFVAs, and Restek_#6 EP Bottle.

3.6 Vacuum Heat Treatment of Cu and ND-Cu Coated CFVAs

Due to the higher than expected H₂ off-gas rates, the Cu and ND-Cu coated CFVA components were vacuum heat treated to extract the hydrogen as indicated in the experimental procedure. In an effort to minimize the number of furnace loads, both Cu and 50% ND-Cu coated CFVA components were placed into one furnace load. They were heated to the 350 °C extraction temperature over 150 hours (5.83 days) and soaked at 350 °C for ~280 hrs (11.6 days). The 25% ND-Cu coated CFVA components were heated to 350 °C over a period of about 74.5 hrs (3.1 days) and soaked at 350 °C for ~124 hrs (5.1 days). The Cu and 50% ND-Cu coated CFVA components took nearly twice as long as that for the 25% ND-Cu coated CFVA components be heated to 350 °C to meet the heating and pressure criteria described in Section 2.3. The CFVA components were thermally soaked until the total pressure at temperature was the same order of magnitude as the room temperature starting pressure. The vacuum extraction profiles for Cu and 50% ND-Cu coated CFVA components (A) and 25% ND-Cu coated CFVA components (B) are shown in Figure 3-12.

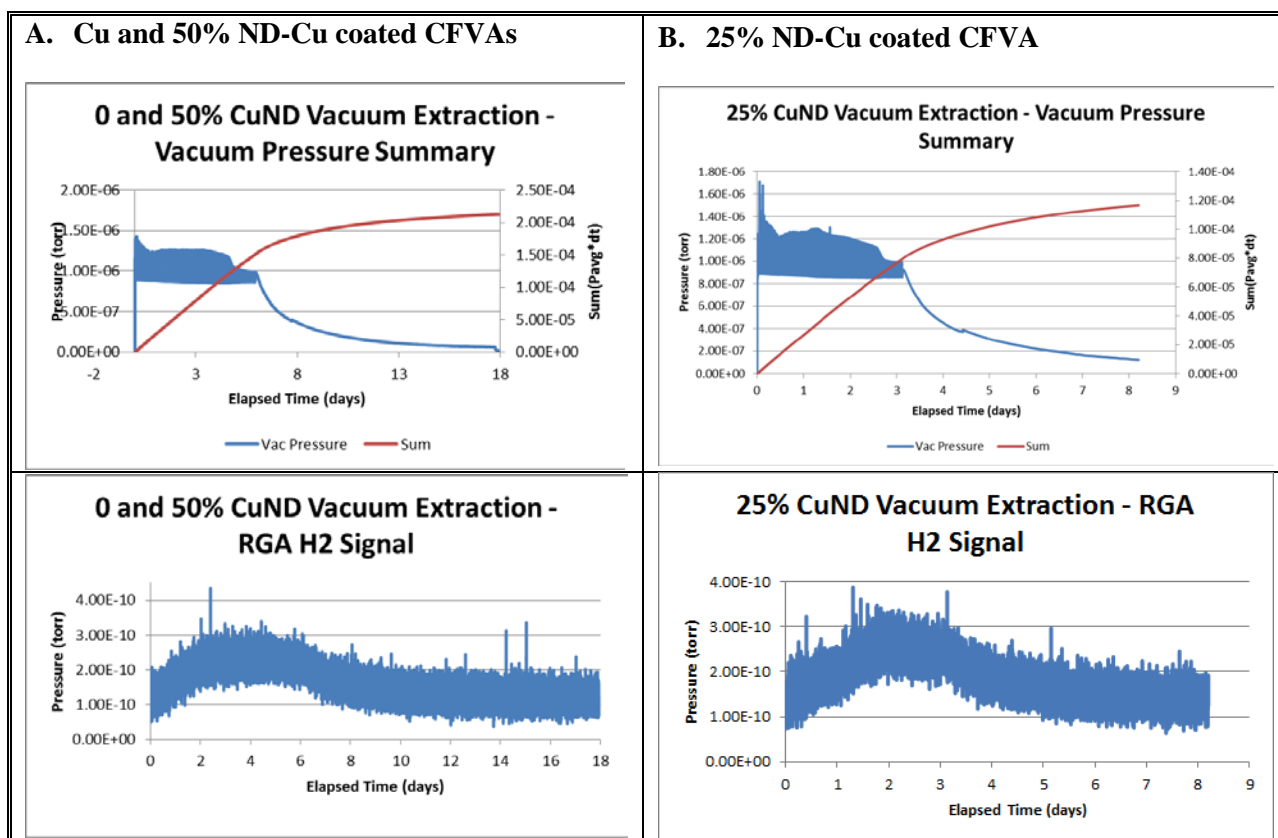


Figure 3-12. The Vacuum Extraction Profiles for Cu and 50% ND-Cu Coated CFVA Components (A) and 25% ND-Cu Coated CFVA component (B).

3.7 Gas Characterization of Vacuum Heated Cu and ND-Cu Coated CFVAs

The CFVA components that were vacuum extracted were assembled with Cu gaskets and SS bolts, and loaded with 500-800 mTorr of deuterium, and the gas composition was monitored and measured using the technique described previously with the MS. The initial off-gas rates were calculated similarly to the as-received CFVAs. The calculated off-gas rate data are provided in Appendix I. The off-gas rates of the most important gas components (i.e., H₂, HD, H₂O, CH₃, N₂, and O₂) for these vacuum treated CFVAs, in comparison with stainless steel (SS) and electropolished (EP) SS CFVAs, and Restek's #6 EP bottle, are presented in Table 3-4 and displayed in Figure 3-13.

Compared to the as-received Cu and ND-Cu coated CFVAs (Table 3-3 and Figure 3-11), the off-gas rates of H₂, HD and H₂O were reduced generally by one to two orders of magnitude after vacuum heating (Table 3-4 and Figure 3-13). At similar sampling times, the off-gas rates of H₂, HD and H₂O for the Cu and ND-Cu coated SS CFVAs (7 days) were at the same order of magnitude as those for SS and EP_SS CFVAs (12 days). For example, the H₂ and HD off-gassing rate of the vacuum heated Cu and Cu-50%ND CFVAs were in the level of 10⁻¹⁴ L mbar/s cm², a value consistent with the untreated stainless steel CFVAs. These results demonstrated that vacuum heating essentially removed the entrapped residual H₂ and adsorbed H₂O for the Cu and ND-Cu coated SS CFVA components, consistent with the hydrogen and total pressure trace shown in Figure 3-12. Based on the lower protium off-gassing after vacuum extraction,

the CFVAs were loaded with an additional 500 mTorr of H₂ after the seven day data set. These samples were then allowed to equilibrate and sampled. The results indicate that the HD formation in the Cu coated CFVA is more rapid than stainless steel.

The off-gas rates of CH₃, N₂ and O₂ for Cu and 50% ND-Cu coated SS CFVAs are similar to those for the untreated SS and EP_SS gas CFVAs, even for the Cu coated CFVA that was monitored up to 70 days. These results indicated that the Cu and 50% ND-Cu coated CFVAs do not exhibit the formation of hydrocarbon species, and there were no air leaks for these CFVAs either.

Overall, the off-gas rates of the monitored gas constituents for the vacuum treated Cu and 50% ND-Cu coated SS CFVAs were nearly as low as those for untreated SS and EP_SS CFVAs. However, compared to the Restek #6 EP bottle, the off-gas rates of all monitored gas components for the vacuum treated Cu and 50% ND-Cu coated SS CFVAs, as well as SS and EP_SS CFVAs, were all much higher. Therefore, based on currently available data, the Restek #6 EP bottle is superior for suppressing hydrogen off-gassing and suppressing the hydrogen and deuterium exchange reaction among all CFVAs we evaluated.

Table 3-4. Off-gas Rates (1 mbar/s cm²) of Vacuum-Treated Cu and ND-Cu Coated CFVAs Tested with D₂ Loadings

CFVAs	Time (Days)	H ₂	HD	H ₂ O	CH ₃	N ₂	O ₂
Cu_SS	7	1.06×10 ⁻¹⁴	3.84×10 ⁻¹⁴	-1.09×10 ⁻¹⁵	4.82×10 ⁻¹⁷	7.36×10 ⁻¹⁵	0.28×10 ⁻¹⁶
50% ND-Cu_SS	7	1.36×10 ⁻¹⁴	6.67×10 ⁻¹⁴	-2.20×10 ⁻¹⁵	3.37×10 ⁻¹⁷	5.66×10 ⁻¹⁵	0.05×10 ⁻¹⁶
SS	12	0.84×10 ⁻¹⁴	1.96×10 ⁻¹⁴	-0.12×10 ⁻¹⁵	0.86×10 ⁻¹⁷	2.16×10 ⁻¹⁵	1.28×10 ⁻¹⁶
EP_SS	12	1.58×10 ⁻¹⁴	2.36×10 ⁻¹⁴	7.04×10 ⁻¹⁵	6.07×10 ⁻¹⁷	2.55×10 ⁻¹⁵	2.24×10 ⁻¹⁶
Restek_#6 EP	12	0.001×10 ⁻¹⁴	-0.0009×10 ⁻¹⁴	0.007×10 ⁻¹⁵	0.05×10 ⁻¹⁷	0.08×10 ⁻¹⁵	0.02×10 ⁻¹⁶
Note: 25% ND-Cu_SS vacuum extracted data were not obtained due to air in-leakage.							

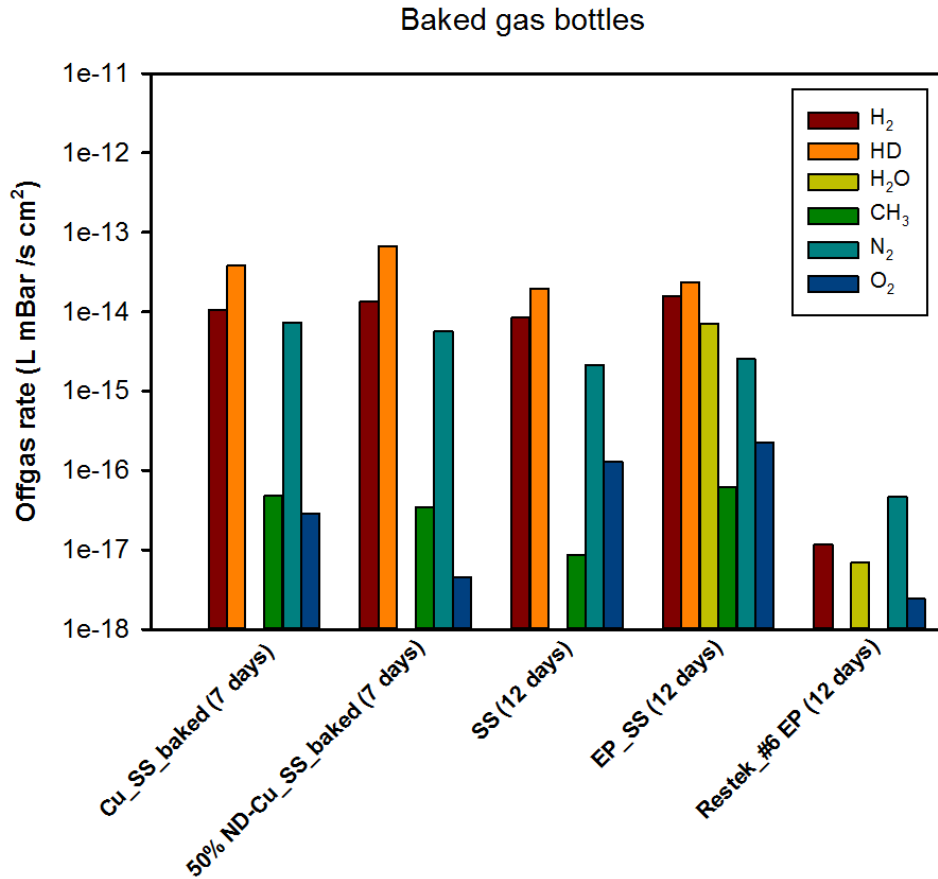


Figure 3-13. Off-gas Rates of the Key Gas Components for Vacuum Treated Cu and 50% ND-Cu Coated CFVAs, in Comparison with SS and EP_SS CFVAs, and Restek_#6 EP Bottle.

After the 7 day pure D₂ exposure, the Cu_SS and 50% ND-Cu_SS CFVAs that had been vacuum treated were loaded with a hydrogen aliquot and the exposure was continued. The gas was sampled and analyzed by MS after 0, 16 and 70 days. The percentages of H₂, HD and D₂ against time were plotted in Figure 3-14, assuming that H₂+HD+D₂ was 1. The data suggests that at 70 days, the mixture in the Cu CFVA was essentially at equilibrium, because at 50:50 of H₂-D₂ mix, the equilibrium ratios for H₂:HD:D₂ is 26:47:26 at 20 °C. A slight increase in the amount of hydrogen was observed, likely due to continued outgassing of the coating, but this was not unexpected. The data set for 50% ND-Cu_SS CFVA appears to reach equilibrium much faster than the pure Cu coated CFVA, but it also appears that hydrogen was still off gassing from this coating and adding hydrogen to the mixture; this increase is especially obvious for the 70 day sample.

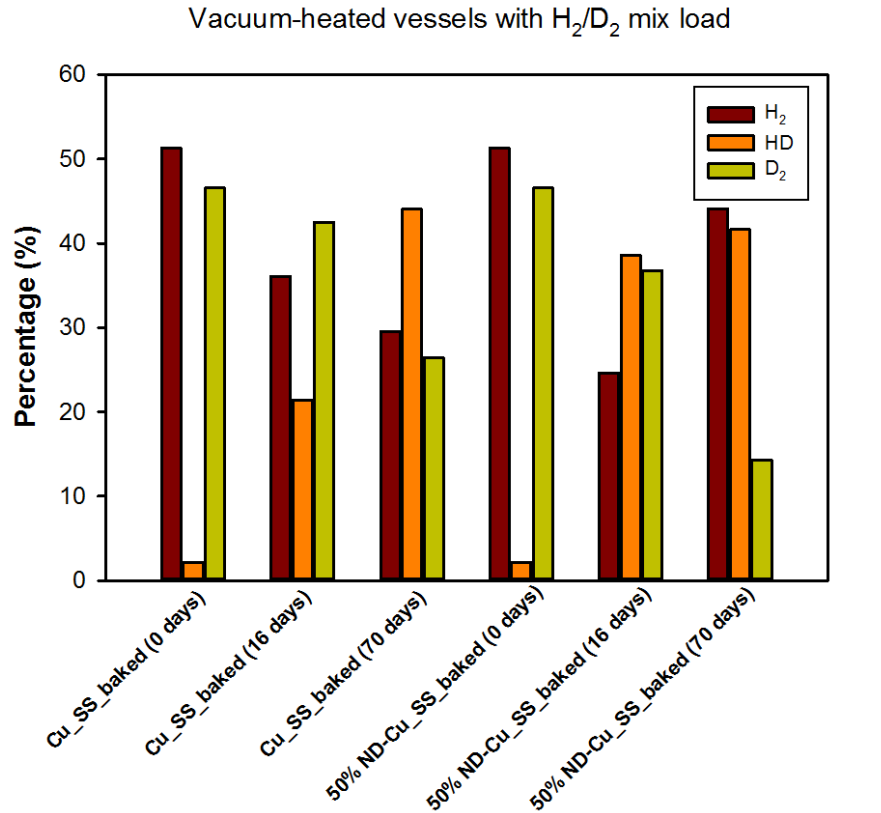


Figure 3-14. Percentages of H₂, HD and D₂ for Vacuum Treated Cu and 50% ND-Cu-Coated CFVAs with H₂-D₂ Mix Load.

4.0 Conclusions

- 1) An electroless plated nanodiamond (ND) coating process was developed to deposit ND and metallic copper matrix on stainless steel parts for surface passivation applications. The type 304L stainless steel assemblies comprised of a 2.75" (DN40) Conflat flanged pipe nipple with a blank flange on one end and a CF to VCR adapter on the other with a nominal volume of 100 mL were plated with diamond loadings of 0%, 25% and 50% v/v in Cu matrix.
- 2) The Cu and ND-Cu coated stainless steel parts were evaluated for surface morphology, composition and ND distribution using microscopy, SEM and EDX. Some areas of the plated stainless steel parts exhibited discoloration and apparent staining. Some pores were observed on the plated parts, but the coating holidays did not extend through the coating to expose the inner stainless steel substrate. The grain size, shape and morphology of the metallic Cu varies with the ND loading: from octahedral shapes in the absence of ND, through spherical deposits in the presence of 25% ND, to spheres and long rods with varying sizes from 5 to 25 μm in the 50% ND-Cu coated flange. The 50% ND-Cu coated flange also exhibited a number of agglomerates of 100 μm or larger in size, and the chemistry of these agglomerates is characterized by Cu and C.
- 3) For as-received Cu and ND-Cu coated CFVAs, hydrogen off-gassing is rapid, and the off-gas rates of H₂, HD and H₂O were one to two orders of magnitude higher than those for both untreated and electropolished stainless steel CFVAs. These results indicated that residual H₂ and H₂O were entrapped in the Cu and ND-Cu coated CFVAs during the plating process, and ND and/or Cu might

facilitate catalytic isotope exchange reaction for HD formation. Hydrocarbons (e.g., CH₃) were not observed and are thus not considered an issue for Cu and ND-Cu coated CFVAs exposed to H₂ and D₂.

- 4) After vacuum treating, residual H₂ and H₂O in Cu and ND-Cu coated CFVAs were dramatically reduced. H₂ and HD off-gassing rates of the vacuum heated Cu and 50% ND-Cu coated CFVAs were on the level of 10⁻¹⁴ 1 mbar/s cm², while H₂O off-gas rate was on the level of 10⁻¹⁵ 1 mbar/s cm², consistent with the untreated or electropolished stainless steel CFVAs.
- 5) Cu and Cu-ND CFVAs loaded with H₂ / D₂ mixtures achieved equilibrium compositions rapidly and the rate was more accelerated in the presence of ND.
- 6) Untreated and electropolished stainless steel CFVAs had hydrogen off-gassing rates that were about two orders of magnitude lower than the as-received Cu and ND-Cu. The Restek EP and SilTek coated bottles had very little hydrogen off-gassing and unmeasurable H₂/D₂ exchange, and exhibited superior performance in H₂/D₂ exposure compared to the stainless steel CFVAs evaluated in this project.

5.0 Recommendations, Path Forward and Future Work

- 1) Cu and ND-Cu coated stainless steel CFVAs did not show an improvement in the H₂, H₂O and HD off-gassing rates compared to untreated or electropolished stainless steel CFVAs. Thus, the electroless plated nanodiamond coating is not considered promising as a surface passivation technology.
- 2) The ND-Cu coating may be beneficial for another application in which catalyzing H₂-D₂ exchange reactions is desired and further experimentation on their suitability as hydrogen cracking should be pursued.

3) References

- [1] ASTM A967, Standard Specification for Chemical Passivation Treatments for Stainless Steel Parts, ASTM International, 100 Barr Harbor Drive, West Conshohocken, PA 2013.
- [2] ASTM B912, Standard Specification for Passivation of Stainless Steels Using Electropolishing, ASTM International, 100 Barr Harbor Drive, West Conshohocken, PA 2013.
- [3] AMS2700, Passivation of Corrosion Resistant Steels, SAE International, 2011.
- [4] Clark, E.A., Evaluation of alternate stainless steel surface passivation methods, WSRC-TR-2005-00246, Savannah River National Laboratory, Westinghouse Savannah River Company, Aiken, South Carolina, 29808, 2005.
- [5] Clark, E.A., Mauldin, C.B., Neikirk, K.C., Evaluation of alternate stainless steel surface treatments for mass spectroscopy and other tritium systems, SRNL-STI-2012-000181, Savannah River National Laboratory, Savannah River Nuclear Solutions, LLC, Aiken, South Carolina 29808, 2012.
- [6] Ajo, H.M., Blankenship, D.W., Clark, E.A., Analysis of passivated surfaces for mass spectrometer inlet systems by Auger electron and X-ray photoelectron spectroscopy, SRNL-STI-2010-00394, Savannah River National Laboratory, Savannah River Nuclear Solutions, LLC, Aiken, South Carolina 29808, 2010.
- [7] Adam, W., Bauer, C., Berdermann, E., Bergonzo, P., Bogani, F., Borchi, E., Brambilla, A., Bruzzi, M., Colledani, C., Conway, J., Dabrowski, W., Delpierre, P., Deneuille, A., Dulinski, W., van Eijk, B., Fallou, A., Fizzotti, F., Foulon, F., Friedl, M., Gan, K.K., Gheeraert, E., Grigoriev, E., Hallewell, G., Hall-Wilton, R., Han, S., Hartjes, F., Hrubec, J., Husson, D., Kagan, H., Kania, D., Kaplon, J., Karl, C., Kass, R., Knöpfle, K.T., Krammer, M., Logiudice, A., Review of the development of diamond radiation sensors, Nuclear Instruments and Methods in Physics Research Section A: Accelerators, Spectrometers, Detectors and Associated Equipment, 434, 131-145, 1999.
- [8] Vatnitskyt, S., Järvinent, H., Application of a natural diamond detector for the measurement of relative dose distributions in radiotherapy, Phys. Med. Biol. 38, 173-184, 1993.
- [9] Dunn, A.R., Duffy, D.M. Stoneham, A.M., A molecular dynamics study of diamond exposed to tritium bombardment for fusion applications, Nuclear Instruments and Methods in Physics Research B 269, 1724–1726, 2011.
- [10] Temmerman, G.De., Doerner, R.P., John, P., Lisgo, S., Litnovsky, A., Marot, L., Porro, S., Petersson, P., Rubel, M., Rudakov, D.L., Van Rooij, G., Westerhout, J., Wilson, J.I.B., Interactions of diamond surfaces with fusion relevant plasmas, T138, Article # 014013, 2009.
- [11] Spencer, W.A., Korinko, P.S., Aluminum and other coatings for the passivation of tritium storage vessels, SRNL-STI-2016-00626, Savannah River National Laboratory, Savannah River Nuclear Solutions, LLC, Aiken, South Carolina 29808, 2016.

Appendix I. Off-gas Rate Datasheet for Cu and ND-Cu Coated Gas CFVAs and Other Reference CFVAs

Notes: All Data scaled to D2 which gave approximately 1E5 counts for 100 microliters of gas equivalent with a surface area of 156 cm2
100 mL bottle surface area is 156 cm2
400mL consistier surface area approximately 400 cm2
leak rate as xxxxxx l mbar/s cm2

Botlle	Time(sec) H	H2+D	H3	HD	D2	HD2	C	HC	N2,CH2	CH3	O2	OH	H2O	HDO	D2O,CD4	CO2++	CH3H	N2,CO	O2	Ar	C3H7	CO2	C4H10
Al#1_100ml	526217.9	1.57E-15	4.89E-14	2.41527E-14	0	-2E-15	5.01E-16	1.36E-16	7.37E-14	1.47E-15	1.61E-14	3.63E-16	1.01E-16	3.23E-16	-3.4E-15	-4.9E-18	5.73E-16	7.01E-13	9.18E-14	6.97E-15	5E-16	1.83E-15	1.67E-16
Al#1_100ml	872512.1	6.64E-16	3.07E-14	1.55632E-15	0	-2.1E-15	1.71E-16	5.92E-17	1.99E-14	6.3E-16	4.13E-15	-1.8E-18	-1.1E-15	-7.1E-16	-4.3E-15	-9.6E-18	2.68E-16	1.8E-13	2.16E-14	1.8E-15	2.48E-16	6.24E-16	9.05E-17
Al#1_100ml	1200950	1.09E-16	3.14E-14	8.1541E-16	0	-8.5E-16	2.92E-16	6.86E-17	2.18E-14	6.4E-16	5.4E-15	6.94E-16	1.43E-15	1.12E-15	-3.5E-15	-4.7E-18	3.02E-16	2E-13	2.81E-14	2E-15	2.64E-16	9.15E-16	3.72E-16
Al#1_100ml	1215172	2.36E-16	1.42E-14	1.04078E-15	0	-4.6E-16	1.33E-16	2.66E-17	1.71E-14	3.78E-16	4.09E-15	-9.6E-17	-1E-15	-7.5E-16	-2.8E-15	-3.3E-18	1.32E-16	1.94E-13	2.31E-14	1.89E-15	1.14E-16	4.15E-16	1.37E-16
Al#2_100ml	1217498	1.13E-15	3.76E-14	2.88875E-14	0	-6.7E-18	1.22E-16	1.51E-16	5.89E-16	1.37E-15	1.59E-15	-6E-17	-7.9E-16	-2E-16	-2.3E-15	-3.2E-18	4.52E-16	3.66E-15	6.54E-17	4.85E-17	3.27E-16	7.17E-16	1.01E-16
CrPlate_100ml	428122.7	7.88E-15	4.87E-13	3.73175E-14	0	6.33E-15	1.57E-16	6.8E-17	1.65E-16	9.33E-17	1.11E-15	1.76E-15	7.51E-15	1.75E-15	-1.2E-14	7.25E-17	1.14E-16	2.9E-15	4.02E-16	7.06E-17	1.04E-16	1.59E-15	6.40E-17
CrPlate_100ml	4118091	4.66E-15	2.06E-13	3.72708E-14	0	1.28E-17	1.03E-16	5.92E-18	7.16E-17	2E-17	3.2E-16	1.4E-15	4.95E-15	2.81E-15	-8.5E-16	4.09E-18	5.24E-17	2.21E-15	1.33E-16	1.84E-17	7.21E-17	6.13E-16	4.07E-17
CrPlate_100ml	8630581	7.51E-16	1.62E-14	2.86524E-14	0	6.75E-17	1.02E-16	6.68E-18	1.71E-14	3.07E-16	4.36E-15	2.7E-16	8.47E-16	6.63E-16	-1.3E-16	4.35E-18	5.37E-17	1.73E-13	2.76E-14	1.78E-15	3.92E-18	5.99E-16	2.66E-18
CrPlate_100ml baked	598314.7	1.03E-15	1.17E-14	6.26423E-14	0	-2.6E-15	4.13E-16	1.3E-17	1.47E-14	2.23E-16	2.57E-15	3.99E-16	-2.3E-15	-3.9E-15	-1.5E-14	-2.1E-17	1.04E-16	1.68E-13	2.3E-14	1.52E-15	5.47E-17	1.53E-15	4.75E-17
CrPlateEP_100ml	430609	6.81E-15	3.79E-13	7.65584E-15	0	2.83E-15	1.93E-16	8.49E-17	2.21E-16	1.69E-16	1.16E-15	2.25E-15	9.42E-15	3.72E-15	-8.7E-15	8.02E-17	1.25E-16	3.85E-15	2.53E-16	1.38E-16	1.26E-16	1.7E-15	1.28E-16
CrPlateEP_100ml	4119328	2.89E-15	1.49E-13	3.27254E-15	0	-2.2E-16	3.77E-17	1.99E-18	4.17E-18	1.13E-17	1.05E-16	6.82E-16	2.19E-15	1.66E-15	-8.4E-16	5.15E-19	4.88E-17	4.5E-16	7.4E-19	4.56E-18	7.16E-17	3.65E-16	2.95E-17
CrPlateEP_100ml baked	596830.9	2.1E-15	1.7E-14	4.11829E-14	0	-1.9E-15	1.16E-15	5E-17	3.76E-14	6.06E-16	8.04E-15	2.07E-15	3.3E-15	-3.3E-15	-1.5E-14	-3.2E-18	3.19E-16	4.32E-13	6.02E-14	4.03E-15	1.43E-16	3.42E-15	1.22E-16
CuSS_100ml	113976E-13	1.13976E-13	0	0	0	-8.9E-16	1.11E-17	1.54E-17	2.21E-16	4.77E-17	-2.6E-16	9.16E-16	-1E-16	9.8E-16	-1.2E-14	-3E-18	1.24E-17	1.45E-15	9.3E-18	2.72E-17	1.03E-18	1.78E-15	2.36E-17
CuSS_100ml	3697805	1.5E-14	7.26E-13	1.06624E-13	0	1.62E-16	2.19E-16	9.18E-18	8.4E-16	6.19E-17	8.96E-16	3.61E-15	1.29E-14	3.79E-15	-1.7E-15	1.89E-17	3.41E-17	1.14E-14	1.21E-15	9.81E-17	8.58E-17	2.65E-15	3.32E-17
CuSS_100ml baked	595588.4	8.34E-16	1.06E-14	3.83548E-14	0	6.24E-15	3.56E-16	1.57E-17	2.64E-16	4.82E-17	2.7E-16	3.47E-16	-1.1E-15	-2.2E-15	-1E-14	-9.6E-18	4.52E-17	7.36E-15	2.84E-17	4.7E-17	5.16E-17	1.67E-15	5.2E-17
CuSS_100ml baked	1365223	1.12E-14	3.9E-13	2.30887E-13	0	-1.3E-15	4E-16	1.39E-17	3.33E-16	3.45E-17	1.48E-15	3.22E-15	1.01E-14	5.95E-15	-4E-15	1.53E-17	6.94E-17	7.22E-15	2.85E-16	7.75E-17	6.18E-17	2.24E-15	5.41E-17
CuSS_100ml baked	6042871	4.22E-15	1.16E-13	1.75286E-13	0	3.25E-16	1.34E-16	5.98E-18	2.16E-16	1.41E-17	2.73E-16	5.28E-16	1.53E-15	1.34E-15	-5.5E-16	5.22E-18	9.32E-18	2.44E-15	4.82E-18	3.07E-17	7.94E-18	9.43E-16	6.16E-18
ND25_100ml	588535	4.1E-14	2.66E-12	1.21301E-13	0	3.71E-16	3.61E-16	7.26E-17	3.77E-16	4.18E-16	2.6E-15	5.09E-15	1.52E-14	1.31E-14	-1E-14	1.42E-16	2.59E-17	8.26E-15	2.38E-17	1.76E-16	2.1E-17	1.46E-14	7.45E-18
ND25_100ml	3697805	2.13E-14	3.26E-12	5.7063E-13	0	1.05E-16	3E-15	8.03E-17	1.3E-15	4.74E-16	8.91E-15	3.19E-14	1.22E-13	1.56E-14	-1.6E-15	3.78E-16	1.09E-16	1.85E-14	1.15E-15	1.55E-16	1.42E-16	4.38E-14	5.99E-17
ND25_100ml	9056253	8.16E-15	3.69E-13	8.99297E-14	0	-8.4E-17	2.03E-16	6.99E-18	1.52E-14	2.49E-16	3.42E-15	1.31E-15	4.37E-15	2E-15	-5.5E-16	1.17E-17	4.81E-17	1.54E-13	1.95E-14	1.52E-15	9.48E-18	1.67E-15	5.27E-18
ND50_100ml	600970.1	8.41E-15	2.64E-13	5.35353E-13	0	-3.3E-15	3.78E-16	2.5E-17	1.3E-16	8.3E-17	1.4E-15	9.89E-17	-6.1E-17	4.19E-16	-9.2E-15	8.98E-17	2.38E-17	1.43E-15	4.68E-17	2E-17	2.29E-17	1.06E-14	1.51E-17
ND50_100ml	3104981	2.51E-14	6.33E-13	5.2577E-13	0	7.22E-16	2.93E-15	4.75E-17	1.64E-15	9.84E-17	8.89E-15	3.57E-14	1.33E-13	2.29E-14	-1.6E-16	3.69E-16	8.87E-17	2.98E-14	3.18E-15	2.36E-16	1.24E-16	4.23E-14	8.36E-17
ND50_100ml baked	598955.2	8.25E-16	1.36E-14	6.66561E-14	0	4.88E-15	3.64E-16	1.16E-17	2.31E-16	3.37E-17	1.87E-16	8.24E-17	-2.2E-15	-2.6E-15	-1.1E-14	-3.7E-18	4.71E-17	5.66E-15	4.48E-18	1.97E-17	4.48E-17	1.94E-15	4.5E-17
SS_100ml	1084732	2.02E-16	8.44E-15	1.96328E-14	0	-1.4E-15	-4.4E-18	7.35E-18	1.04E-16	8.55E-18	9.85E-17	-2.9E-17	-1.2E-16	-3.5E-16	-1.3E-15	-1.1E-18	-3.8E-18	2.14E-15	1.28E-16	2.96E-17	1.22E-18	5.18E-16	-6.3E-19
SS_100ml	4664777	9.47E-16	2.2E-14	4.7942E-14	0	1.59E-17	4.96E-17	1.95E-18	4.78E-16	9.37E-18	1.44E-16	2.81E-16	7.54E-16	1.04E-16	-1.2E-15	1.78E-18	8.22E-18	6.27E-15	5.24E-16	6.04E-17	1.13E-17	4.59E-16	1.04E-17
SS_EP_100ml	1032981	7.29E-16	1.58E-14	2.36185E-14	0	-2.8E-16	1.53E-16	4.79E-17	6.07E-17	8.41E-16	9.04E-16	7.04E-15	3.72E-15	2.51E-15	6.41E-17	5.78E-17	4.20E-17	2.59E-15	2.24E-16	5.57E-17	5.22E-17	9.61E-16	3.5E-17
SS_EP_100ml	4663792	7.13E-16	1.09E-14	3.96994E-14	0	-2.4E-16	3.73E-17	1.33E-18	8.86E-17	5.82E-18	9.13E-17	2.76E-16	8.21E-16	2.99E-16	-7E-16	5.91E-19	7.09E-18	1.6E-15	1.7E-16	1.49E-17	9.11E-18	2.96E-16	7.45E-18
restek_#5_siltek	1029253	-4E-17	-7.7E-16	-2.63105E-16	0	-5.4E-16	-1.2E-17	6.17E-19	-3.1E-18	2.55E-18	2.93E-18	4.48E-17	-9.3E-18	-1.5E-16	-4.7E-16	-2E-18	1.18E-19	-1.6E-16	-5.5E-19	1.88E-18	-1.2E-18	-4E-17	-7.8E-19
restek_#5_siltek	4591425	9.05E-18	-4.5E-17	-1.13098E-16	0	-2.2E-16	4.91E-18	3.65E-19	-7.3E-20	1.46E-18	-1.9E-17	1.81E-17	-1.1E-16	-2.1E-16	-7.8E-16	-1.6E-18	2.35E-18	7.91E-17	-1.2E-18	4.22E-19	3.38E-18	3.43E-17	3.16E-18
restek_#6EPSS	9599036	7.67E-18	6.62E-17	-1.80966E-17	0	1.37E-17	5.47E-18	1.97E-19	1.03E-18	4.42E-19	1.66E-17	1.07E-17	4.4E-19	-5E-18	-1.6E-16	-1.9E-19	6.79E-19	7.99E-17	2.76E-18	5.76E-19	5.1E-19	2.5E-17	1.97E-18
restek_#6EPSS	1031848	2.04E-15	3.58E-16	-1.71505E-16	0	-2.1E-15	5.72E-16	3.75E-17	1.63E-16	1.61E-15	2.04E-15	1.46E-14	2.6E-15	-9.7E-16	8.81E-17	2.97E-16	5.97E-15	-2E-18	1.78E-16	2.02E-16	-2.3E-17	9.44E-18	1.19E-20
restek_#6EPSS	4599420	-1.9E-17	-1.8E-16	-5.3653E-17	0	-7.4E-17	-3.5E-18	6.44E-20	-8.3E-19	4.99E-19	-4.1E-18	-3.4E-18	-4.3E-17	-6.6E-17	-1.2E-16	-4.7E-19	-2.1E-19	-3.9E-17	-1.2E-18	3.88E-19	-3.4E-19	-9.6E-18	1.19E-20
restek_#6EPSS	9599036	1.79E-18	-6.1E-17	3.64452E-17	0	-1.1E-16	1.28E-18	1.28E-19	-1E-19	4.97E-19	-1E-17	4.34E-18	-7E-17	-9.9E-17	-3.7E-16	-8E-19	7.08E-19	2.24E-17	-7.6E-19	3.35E-19	1.21E-18	1.2E-17	1.39E-18
restek_#6EPSS	1271737	6.29E-18	1.18E-17	-9.28419E-18	0	2.68E-17	5.28E-18	1.94E-19	9.13E-19	4.79E-19	1.71E-17	1.51E-17	6.91E-18	-7.4E-18	-1.6E-16	-2.7E-19	7.4E-19	7.63E-17	2.4E-18	7.26E-19	4.94E-19	2.51E-17	3.87E-19

Distribution:

B.A. Ferguson, 235-H
R.W. Allgood Jr., 246-1H
T.J. Worrell, 246-1H
C.B. Mauldin, 246-2H
M.L. Whitehead, 246-2H
C.D. Blair, 246-2H
C.M. Gregory, 773-A
M.A. Collins, 246-1H
K.L. Session, 246-1H
C.F. Swanson II, 246-1H
C.W. Gardner, 772-F
C.M. Crawford, 235-H
D.W. Bickley, 246-2H
C.L. Reville, Jr., 264-1H
K.M. Cross, 264-1H
R.P. Addis, 773-A
M.J. Barnes, 773-A
D.W. Babineau, 999-2W
J.E. Halverson, 999-2W
D. Li, 773-42A
P.S. Korinko, 999-2W
W.A. Spencer, 999-2W
E. Stein, 999-2W
S.M. Serkiz, 999-2W
R.B. Wyrwas, 999-2W
D.I. Kaplan, 773-42A
J. J. Mayer, 999-W
Records Administration (EDWS)